

Electronic spectra of linear HC₅H and cumulene carbene H₂C₅

Mathias Steglich,^{1, a)} Jan Fulara,^{1, 2} Surajit Maity,¹ Adam Nagy,¹ and John P. Maier^{1, b)}

¹⁾Department of Chemistry, University of Basel, Klingelbergstrasse 80, CH-4056 Basel, Switzerland

²⁾Institute of Physics, Polish Academy of Sciences, Al. Lotników 32/46, PL-02-668 Warsaw, Poland

The $1^3\Sigma_u^- \leftarrow X^3\Sigma_g^-$ transition of linear HC₅H (**A**) has been observed in a neon matrix and gas phase. The assignment is based on mass-selective experiments, extrapolation of previous results of the longer HC_{2n+1}H homologues, and density functional and multi-state CASPT2 theoretical methods. Another band system starting at 303 nm in neon is assigned as the $1^1A_1 \leftarrow \tilde{X}^1A_1$ transition of the cumulene carbene pentatetraenylidene H₂C₅ (**B**). (published in *J. Chem. Phys.* 142 (2015) 244311)

I. INTRODUCTION

Unsaturated hydrocarbon chains and their cyano-substituted analogues take part in astrochemical processes as many of them have been detected in different astrophysical environments, such as dense and diffuse clouds or circumstellar shells. On earth, they play major roles as intermediates in combustion and plasma chemistry as well as in other soot-forming processes. The hydrogen-capped HC_nH linear chains are important members of these compounds. They possess no permanent dipole moment and can therefore only be detected via vibrational or electronic spectroscopic methods. For instance, the presence of the even-numbered polyacetylenes HC_{2n}H ($n = 1 - 3$) in stellar outflows and planetary atmospheres was inferred from observations in the infrared.¹⁻⁴ The odd-numbered counterparts are more difficult to synthesize and study in the laboratory because of their open-shell character. They have to be embedded in collision-free environments, i.e., low-temperature matrices or supersonic jets. Their presence in space, albeit yet unproven, is suggested from astronomical detections of linear analogues, such as C_n ($n = 3, 5$) and HC_n ($n = 3, 5, 7$).⁵⁻¹⁰

Within this context, studies of the first allowed electronic transition $1^3\Sigma_u^- \leftarrow X^3\Sigma_g^-$ of the HC_{2n+1}H series, situated in the visible or near-infrared, are of relevance. Respective absorption spectra for chains containing up to 19 carbon atoms have been measured in neon matrices ($n = 2 - 7, 9$) and in the gas phase by resonant two-color two-photon ionization (R2C2PI; $n = 3 - 6, 9$) and cavity ring down spectroscopy (CRDS; $n = 3 - 6$).¹¹⁻¹⁴ Attempts to measure the $1^3\Sigma_u^- \leftarrow X^3\Sigma_g^-$ transition for the smallest members HC₃H and HC₅H in the gas phase failed so far. Whereas the two C₃H₂ isomers with C_{2v} symmetry, which are more stable, were studied¹⁵⁻¹⁹ arguments were given for the non-observation of the electronic transition of HC₅H, including low oscillator strength and unfavorable production conditions.¹³

Several low-energy isomers of C₅H₂ were investi-

gated by quantum chemistry and microwave absorption spectroscopy.²⁰⁻²⁵ Coupled-cluster calculations suggest pentadiynylidene (linear HC₅H triplet; **A**) to be the most stable structure, albeit singlet ethynylcyclopropenylidene (c-HC₃-C₂H; **D**) is close in energy (8 kJ/mol) and three others (**B**, **C**, **F**; see Fig. 1) have been found within 90 kJ/mol.²⁰ Rotational spectra were recorded for the four lowest singlet isomers possessing a permanent dipole moment, i. e., structures **B**, **C**, **D**, **F**,²³⁻²⁵ whereas the HC₅H triplet was studied in solid matrices only.^{11,26} The first matrix investigation was realized by co-authors of this paper.¹¹ Mass-selected C₅H₂ cations produced in a diacetylene discharge were deposited in cryogenic neon; the linear triplet was subsequently generated by photo-induced neutralization and the electronic absorption spectrum was recorded. In a later study by Bowling et al.,²⁶ HC₅H was created by photolysis of diazopentadiyne in a nitrogen matrix; its structure was characterized by IR, EPR, and UV-vis spectroscopy. Inconsistencies between both data sets require a re-investigation of the $1^3\Sigma_u^- \leftarrow X^3\Sigma_g^-$ transition.

This article reports the $1^3\Sigma_u^- \leftarrow X^3\Sigma_g^-$ spectrum of mass-selected HC₅H (**A**) deposited in solid neon with lower kinetic energy and higher mass-resolution than before. A second absorption system commencing at 303 nm is observed and assigned as the $1^1A_1 \leftarrow \tilde{X}^1A_1$ transition of pentatetraenylidene H₂C₅ (**B**). Due to band shifts and broadening, electronic spectra of matrix-isolated molecules can not usually be compared with astronomical data for identification purposes. The gas phase detection and R2C2PI characterization of **A** is reported here for the first time. Vibrational frequencies and rotational constants are obtained.

II. METHODS

A. Experimental

Two types of experiments, in neon matrix and gas phase, were carried out. The apparatus used for the former combines mass spectrometry with matrix isolation. It is described elsewhere.²⁷ The $m/z = 62$ ions were produced in a hot cathode discharge source using different

^{a)}Electronic mail: m.steglich@web.de

^{b)}Electronic mail: j.p.maier@unibas.ch

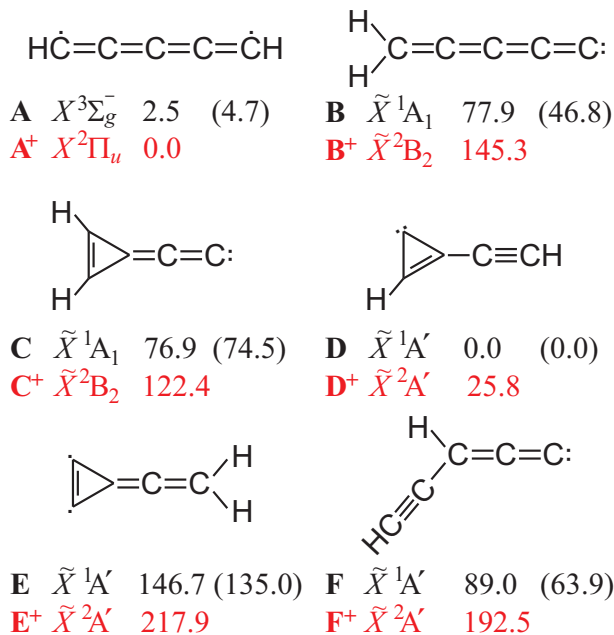


FIG. 1. Zero-point corrected ground state energies (kJ/mol) of neutral isomers of C_5H_2 (black) and their cations (red) at the M06-2X/cc-pVTZ level of theory. Energies calculated at the MS(4)-CASPT2/cc-pVTZ level are given in parentheses.

precursors seeded in helium, such as methyldiacetylene, a mixture of propyne and acetylene, or propyne and diacetylene. Ions extracted from the source were guided to a quadrupole mass filter. Mass-selected C_5H_2^+ was co-deposited with neon forming a 150 μm thick matrix containing cations as well as neutrals. The largest C_5H_2^+ current of about 10 nA was obtained from the methyldiacetylene precursor. Absorption spectra were measured by passing broad band light from a halogen or a high-pressure xenon lamp through the matrix, dispersing the light by a 0.3 m spectrograph, and recording the signal with a CCD camera. Absorptions from neutrals and cations could be discriminated by further irradiation with UV photons ($\lambda > 260$ nm) leading to enhanced C_5H_2 formation.

Gas phase spectroscopy was realized by a resonant two-color two-photon ionization scheme (R2C2PI) on a molecular beam of C_5H_2 and other hydrocarbons. A gas mixture of 0.1 % propyne (C_3H_4) and 0.1 % diacetylene (C_4H_2) in helium discharged in the expansion of a pulsed valve (8 bar backing pressure) provided the target species. Longer homologues of the HC_{2n+1}H series were also observed, their low-resolution (0.1 nm) spectra being identical to those published previously.¹⁴ A collimated beam was produced by a skimmer placed 50 mm downstream. The ions generated by the R2C2PI process were monitored as a function of scanning laser wavelength with a linear time-of-flight mass spectrometer. Spectral scans were undertaken by counter-propagating the radiation of the laser into the molecular beam. An optical parametric

laser (5-10 ns; 20 Hz; 0.1 nm bandwidth) provided photons for broad range scans between 410 and 710 nm. Measured spectra were corrected for wavelength-dependent laser power variations. Higher-resolution scans around 430 nm were conducted with a dye laser (≈ 10 ns; 10 Hz; 0.001 nm bandwidth). The accuracy of the calibration using a wavemeter is ± 0.05 cm^{-1} . An ArF excimer laser emitting 193 nm photons (≈ 10 ns) perpendicular to the beam ionized the molecules.

B. Computational

To assign the C_5H_2 UV features seen in a neon matrix, the six lowest energy isomers depicted in Fig. 1 were selected for a computational study, whereby structures **A**, **B**, **C**, **D**, **F** have been investigated by coupled cluster theory before.²⁰ As starting point for high-level calculations using a multi-configurational second order perturbation theory (CASPT2), equilibrium geometries were first optimized at DFT level (density functional theory) with the M06-2X functional²⁸ and the cc-pVTZ basis^{29,30} set of the Gaussian09 software.³¹ The thus obtained structures were then refined with the CASPT2 method of the MOLCAS program³² along with the same basis set. The reference wavefunction was optimized for the average electronic energy of four electronic states of a given symmetry (multistate option MS(4)). Ten electrons distributed over ten orbitals (10/10) formed the active space. The obtained ground state energies of neutrals and cations are given in Fig. 1. The relative stabilities are comparable to the coupled cluster approach,²⁰ except for a reversed order of the almost isoenergetic HC_5H triplet and $c\text{-HC}_3\text{-C}_2\text{H}$ singlet. Vertical excitation energies of isomers **A–F** were calculated at the MS(4)-CASPT2 (10/12) level. Adiabatic excitation energies have been computed for selected electronic states using MS(4)-CASPT2 (10/10). In addition, electronic transitions were predicted with the symmetry adapted cluster/configuration interaction (SAC-CI) method^{33,34} and the cc-pVTZ basis set of Gaussian09. Vibrational progressions of chosen C_5H_2 transitions and the rotational profile of linear HC_5H were simulated using the PGO-PHER program.³⁵ For this, geometries and vibrations in ground and excited states were predicted with the B3LYP functional^{36,37} and cc-pVTZ basis set using Gaussian09's DFT and time-dependent DFT methods.

III. RESULTS AND DISCUSSION

A. Matrix spectrum of HC_5H

Deposition of $m/z = 62$ ions in a 6 K neon matrix leads to absorptions identical with those reported for linear HC_5H^+ .³⁸ Weak features with onsets at about 430 and 303 nm gained intensity during UV irradiation. They are therefore associated with neutral species. The 430 nm

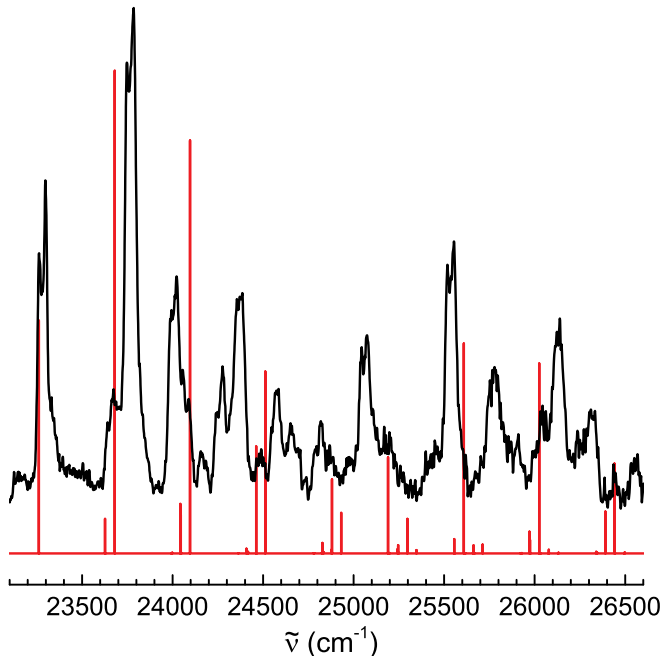


FIG. 2. $1^3\Sigma_u^- \leftarrow X^3\Sigma_g^-$ spectrum of HC_5H in a 6 K neon matrix compared to a Franck-Condon simulation at the B3LYP/cc-pVTZ level ($T_{\text{vib}} = 0$ K).

system is displayed in Fig. 2. It differs from the HC_5H neon matrix spectrum published earlier.¹¹ Back then, absorptions in the 400 – 435 nm range were assigned to the $1^3\Sigma_u^- \leftarrow X^3\Sigma_g^-$ transition of the linear triplet based on mass-selection and the approximate wavelength of the origin band deduced from the positions of the longer HC_{2n+1}H homologues. The most intense bands observed here were also present in the old spectrum, but a stronger absorption system starting at 434 nm assigned recently³⁹ to $\text{H}_2\text{C}_5\text{H}$ overlapped the $1^3\Sigma_u^- \leftarrow X^3\Sigma_g^-$ transition. This radical was absent in the present investigation because of a better mass resolution and a lower kinetic energy of deposited ions. The correct origin band is now observed at 429.9 nm (instead of 434 nm). The difference could be the reason why Ball et al.¹³ were unable to observe HC_5H in their high-resolution study.

The vertical excitation energy of **A** calculated at the MS(4)-CASPT2(10/12)/cc-pVTZ level is 3.28 eV ($f = 0.005$), quite far away from the measured position of the origin band at 2.88 eV. A considerable deformation of the chain structure is obtained upon geometry optimization of the excited $1^3\Sigma_u^-$ state using MS(4)-CASPT2(10/10). The C–C–H angle is subject to the largest distortion and deviates by about 40° from linearity. The adiabatic excitation energy is 2.85 eV, which is much closer to the origin band position and comparable to results from a multi-reference single and double excitation configuration interaction method locating the $1^3\Sigma_u^- \leftarrow X^3\Sigma_g^-$ transition at 2.76 eV ($f = 0.007$).²² No further transition with

appreciable oscillator strength is predicted below 6 eV, but another (dark) $^3\Sigma_u^+$ state is expected in the vicinity of $1^3\Sigma_u^-$. The energetic order of these two states is unknown.

Several vibronic bands in the matrix spectrum show site splitting into doublets of 30 to 40 cm^{-1} energy difference. The band positions measured at the maximum absorption and assignments based on DFT and CASPT2 calculations are summarized in Table I. Some old assignments¹¹ have been corrected in light of the new results. A Franck-Condon simulation of the $1^3\Sigma_u^- \leftarrow X^3\Sigma_g^-$ transition at the B3LYP/cc-pVTZ level is compared with the matrix absorption spectrum in Fig. 2. The computed intensity pattern agrees reasonably well with the observed spectrum, the band positions differ to a larger extent, though. At this level of theory, the fully relaxed excited state structure exhibits C_2 symmetry with a C–C–H angle of about 153° on both ends. The carbon frame is slightly wavy; the average C–C distance has increased by about 1.2% compared to the ground state. This implies that the Franck-Condon active vibrations are C–H bending, C–C chain bending, and C–C stretching modes. The strongest band is predicted to be caused by the single excitation of a C–H bending vibration of A symmetry calculated at 417 cm^{-1} . Due to symmetry difference this vibration cannot directly be mapped to a ground state one. Strong Duschinsky mixing is active; the 417 cm^{-1} mode projects on both C–H bendings $\nu_4(\pi_g)$, $\nu_9(\pi_u)$ of the ground state. For reasons of simplification, the observed bands are labeled within the framework of the ground state, i.e., the strong band at 23747 cm^{-1} is assigned as 4_0^1 . The vibrational energy of 486 cm^{-1} is somewhat higher than the calculated value. Higher-order assignments (two or more quanta) are rather tentative; the potential for the C–H bending seems to be highly anharmonic. The C–C chain bending and stretching modes $\nu_5(\pi_g)$ and $\nu_2(\sigma_g)$ appear at 380 and 1770 cm^{-1} in the excited electronic state in a neon matrix. The computed values in $1^3\Sigma_u^-$ are 367 and 1929 cm^{-1} , respectively. The $\nu_2(\sigma_g)$ mode is better reproduced with 1825 cm^{-1} at the MS(4)-CASPT2(10/10) level.⁴⁰ The 3_0^1 assignment is also tentative due to low Franck-Condon intensity and potential overlap with the $4_0^1 5_0^1$ band. The C–C stretching mode $\nu_3(\sigma_g)$ is calculated at 767 cm^{-1} (CASPT2: 755 cm^{-1}), and possibly measured at 801 cm^{-1} .

B. Gas phase spectrum of HC_5H

The $1^3\Sigma_u^- \leftarrow X^3\Sigma_g^-$ R2C2PI spectrum measured in the gas phase with 0.1 nm laser bandwidth is shown in Fig. 3; the inset is a higher-resolution recording (0.001 nm) of the origin band at 23261 cm^{-1} along with a simulated profile at the B3LYP/cc-pVTZ level. The gas phase position of the origin band is identical to the wavenumber of the lower-energy site in the neon matrix. Quite unusually, a blue shift of 5 to 52 cm^{-1} is observed in

TABLE I. Observed absorption bands (cm^{-1}) in the $1^3\Sigma_u^- \leftarrow X^3\Sigma_g^-$ electronic spectrum of HC_5H .

Ne matrix		Gas phase		Assignment
$\tilde{\nu}$	$\Delta\tilde{\nu}$	$\tilde{\nu}$	$\Delta\tilde{\nu}$	
		23170	-91	$4_1^1 5_1^1$
		23202	-59	5_1^1 or 4_1^1
		23234	-27	4_1^1 or 5_1^1
23261	0	23261	0	0_0^0
23299	38			0_0^0
		23474	213	?
23641	380	23624	363	5_0^1
23674	413			5_0^1
23747	486	23742	481	4_0^1
23787	526			4_0^1
		23958	697	?
23998	737	23975	714	5_0^2
24027	766			5_0^2
24062	801	24050	789	3_0^1
24091	830			3_0^1
24160	899	24149	888	$4_0^1 5_0^1$
24184	923			$4_0^1 5_0^1$
24242	981	24228	967	4_0^2
24278	1017			4_0^2
		24272	1011	?
		24295	1034	?
24355	1094	24334	1073	5_0^3
24390	1129	24349	1088	5_0^3
24576	1315			$3_0^1 4_0^1$
24655	1394			4_0^3
24820	1559			3_0^2
25031	1770			2_0^1
25075	1814			2_0^1
25435	2174			$2_0^1 5_0^1$
25517	2256			$2_0^1 4_0^1$
25556	2295			$2_0^1 4_0^1$
25780	2519			$2_0^1 3_0^1 / 2_0^1 5_0^2$
26137	2876			$2_0^1 4_0^2$
26323	3062			$2_0^1 3_0^1 4_0^1$

neon compared to the gas phase for the other bands and matrix sites. The longer HC_{2n+1}H members experience red-shifts in neon that increase with chain length.^{11,13,14} Three hot bands to the red of the origin band, assigned as 4_1^1 , 5_1^1 , and $4_1^1 5_1^1$, are discernible in the gas phase spectrum. The vibrational temperature is estimated at about 350 K. In addition to the other bands already observed in neon, four weak, yet unidentified features were found by R2C2PI. Their broadness might mask them in the matrix.

The rotational profile of the origin band is very simi-

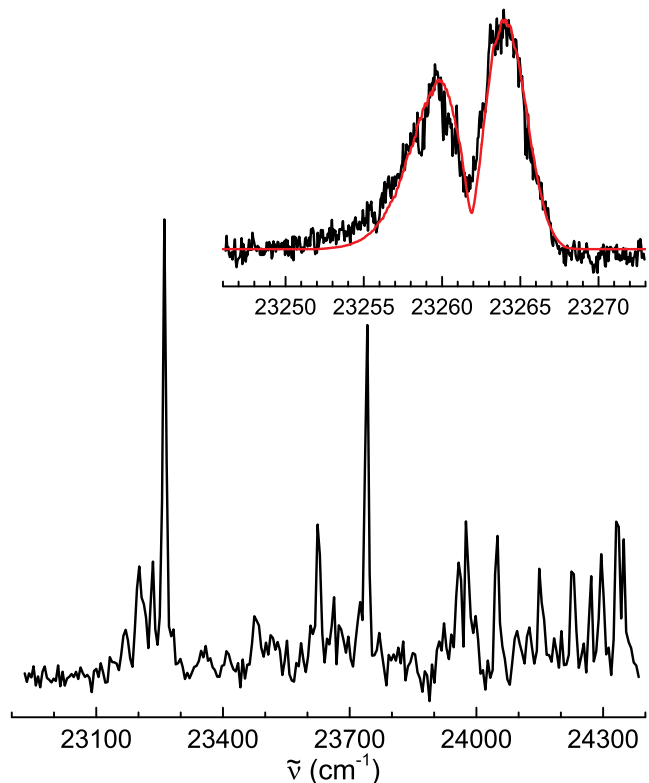


FIG. 3. Gas phase $1^3\Sigma_u^- \leftarrow X^3\Sigma_g^-$ spectrum of HC_5H (0.1 nm laser bandwidth). Inset: origin band (0.001 nm resolution; black trace) and calculated rotational profile ($T_{rot} = 40$ K; red).

lar to those of the longer HC_{2n+1}H homologues,¹³ except for its width, which is circa two times broader. It is satisfactorily explained by the calculated rotational constants in the ground and excited state. Theoretical values at the B3LYP and CASPT2 levels are very similar and lie within the error margins of those ones that were determined by a least squares fit (Table II). The rotational temperature is about 40 K. Spin-spin splitting effects are not discernible. Individual rotational lines are also not resolved. The Lorentzian line width is around 0.5 cm^{-1} , corresponding to an upper electronic state lifetime of 0.1 ps. This is much shorter than the jitter between both lasers used (~ 40 ns). Resonance enhanced ionization can only be achieved if after excitation by the scan laser the molecule relaxes within 0.1 ps to another long-lived state ($\gtrsim 40$ ns) above the ground one.

C. Matrix spectrum of H_2CCCC

The other absorption system in a neon matrix commences at 303 nm (4.1 eV) and is composed of five broad bands with FWHM of about 450 cm^{-1} (Fig. 4). It is about twenty times stronger than the 430 nm HC_5H system. Attempts to measure the corresponding R2C2PI

TABLE II. Spectroscopic constants (cm^{-1}) in the $X^3\Sigma_g^-$ and $1^3\Sigma_u^-$ electronic states of HC_5H .

	Calculation		Fit of 0_0^0
	B3LYP	CASPT2	
$\tilde{\nu}_{00}$	28339	22984	23261.8 ± 0.3
B'_v	0.0761	0.0753	0.0758 ± 0.0004
B''_v	0.0754	0.0746	0.0749 ± 0.0004

spectrum failed. Intense electronic transitions are not expected for the linear triplet around 4.1 eV (Table III). Another C_5H_2 isomer is likely the carrier. The first strong transitions of isomers **B**, **C**, **D**, and **F** are calculated in proximity of the observed absorption energy. Franck-Condon simulations of these transitions were conducted at the B3LYP/cc-pVTZ level. They are compared with the measured spectrum in Fig. 4. In terms of stability, isomer **D** (= ethynylcyclopropenylidene) and its precursor in the matrix experiment, the **D**⁺ cation, are close in energy to **A** and **A**⁺ (see Fig. 1). However, strong excitation of C–H bending vibrations is predicted to result in a long and congested progression in contradiction to the observations. Furthermore **D**⁺ has a calculated transition in the visible with about the same intensity as that of the neutral, which was not observed (Table IV). The only cationic absorption system that could be detected in the matrix before neutralization was that of **A**⁺. The carrier of the 303 nm features, if produced via photo-induced neutralization, must have a cationic form with none or weak absorptions in the monitored 260–1100 nm wavelength range.

The best match between computed Franck-Condon intensities and the observed vibrational progression is provided by the $1^1A_1 \leftarrow \tilde{X}^1A_1$ transition of pentatetraenylidene (**B**). It has an oscillator strength of $f = 0.12$ at the CASPT2 level, while the **B**⁺ cation absorbs only weakly ($f < 0.01$) below 6 eV (Table IV). As demonstrated recently, the $\text{H}_2\text{C}_5\text{H}^+$ cation is efficiently produced from the methyldiacetylene precursor in the same ion source.³⁹ **B**⁺ is easily generated by C–H bond cleavage from $\text{H}_2\text{C}_5\text{H}^+$. Moreover, **B** and **B**⁺ can also be formed from **A** and **A**⁺ *via* hydrogen migration during the trapping of mass-selected ions. It was recently shown for C_7H_3 that this is a feasible process.⁴¹ Therefore the 303 nm system is concluded to be caused by the afore-mentioned transition of the cumulene carbene H_2C_5 . Considering the calculated oscillator strengths and observed absorption intensities, **A** and **B** had about the same abundances in the matrix.

The proposed band assignments are listed in Table V. The progression is mainly caused by excitations of C–C stretching vibrations $\nu_3(a_1)$ and $\nu_6(a_1)$. Band widths are around 200 cm^{-1} , corresponding to the excited electronic state lifetime of about 30 fs. Calculated vibrational frequencies in excited electronic states are not expected to be as accurate as ground state ones. At the

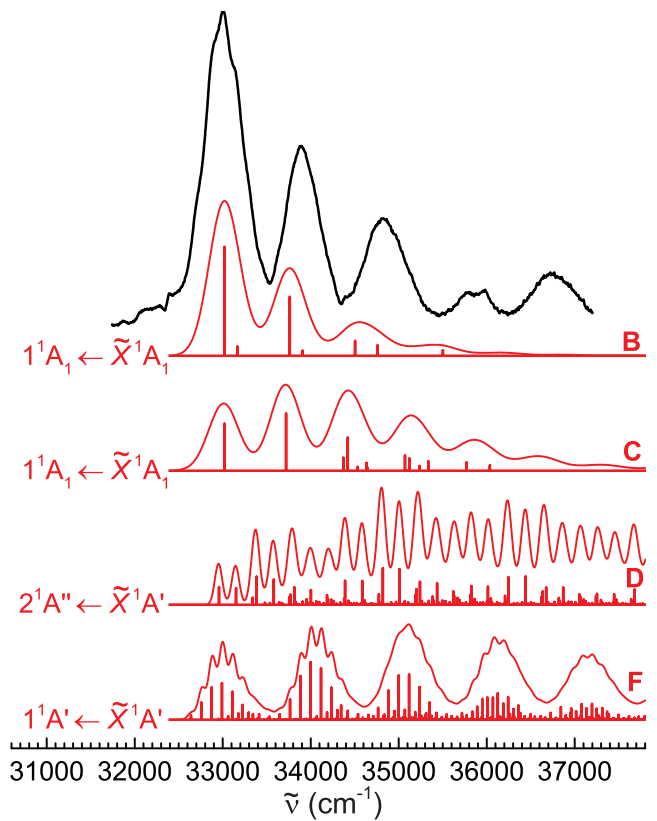


FIG. 4. C_5H_2 absorption spectrum in a neon matrix (black trace) in comparison to Franck-Condon simulation for different isomers at the B3LYP/cc-pVTZ level ($T_{\text{vib}} = 0 \text{ K}$; red traces).

B3LYP/cc-pVTZ level, $\nu_3(a_1)$ and $\nu_6(a_1)$ deviate from observed values by -17% and -5% , respectively. The Franck-Condon approximation often underestimates the intensities of combination bands. This is also noticed here for the bluest observed band at 36740 cm^{-1} . A faint shoulder is recognizable on the high energy side of the origin band. It is assigned to the double excitation of the in-plane C–H₂ bending mode $\nu_{15}(b_2)$.

IV. SUMMARY

The $1^3\Sigma_u^- \leftarrow X^3\Sigma_g^-$ transition of HC_5H has been re-measured in a neon matrix and band assignments have been revised. The respective gas phase spectrum has been observed by R2C2PI for the first time. C_5 and HC_5 have already been found in the circumstellar shell of the carbon star CW Leonis and the Taurus molecular cloud 1.^{7,9,42} A detection of HC_5H might be accomplished with the present data, but the theoretical oscillator strength is only 5×10^{-3} . The $1^3\Sigma_u^- \leftarrow X^3\Sigma_g^-$ transition is characterized by a bent excited state structure, resulting in a vibrational progression with strong contribution from a C–H bending mode. The smaller propargylene diradi-

TABLE III. Calculated electronic transitions of C_5H_2 isomers below 6 eV.

State	SAC-CI		CASPT2 ^a	
	[eV]	<i>f</i>	[eV]	<i>f</i>
A $\tilde{X}^3\Sigma_g^-$				
$1^3\Sigma_u^-$	3.93	0.063	3.28 (2.85)	0.005
$2^3\Sigma_u^-$	5.46	0.002	4.76	0.0000
B \tilde{X}^1A_1				
1^1A_1	3.73	0.15	4.00 (3.87)	0.12
2^1A_1	5.80	0.022	5.02	0.0004
1^1B_1	2.41	0.006	2.03	0.004
2^1B_1	>6.0		4.99	0.009
1^1B_2	5.78	0.031	5.52	0.024
C \tilde{X}^1A_1				
1^1A_1	4.87	0.23	4.65 (4.51)	0.22
1^1B_1	3.50	0.014	3.21	0.012
1^1B_2	5.07	0.019	4.77	0.010
D \tilde{X}^1A'				
$1^1A'$	5.82	0.028	5.82	0.020
$1^1A''$	3.22	0.001	3.24	0.001
$2^1A''$	4.48	0.018	4.66 (4.41)	0.025
E \tilde{X}^1A'				
$1^1A'$	3.46	0.020	3.58 (2.33)	0.024
$2^1A'$	4.57	0.022	4.67	0.010
$1^1A''$	2.60	0.001	2.44	0.002
$2^1A''$	2.87	0.003	3.01	0.004
$3^1A''$	4.90	0.0000	5.08	0.0003
$4^1A''$	>6.0		5.54	0.001
F \tilde{X}^1A'				
$1^1A'$	4.27	0.36	4.35 (4.23)	0.33
$2^1A'$	6.07	0.023	5.69	0.025
$1^1A''$	1.54	0.0000	1.76	0.0001
$2^1A''$	2.30	0.007	2.10	0.0047
$3^1A''$	4.15	0.0000	4.32	0.0001

^a vertical energies at MS(4)-CASPT2(10/12);
adiabatic ones in brackets at MS(4)-CASPT2(10/10)

cal, HC_3H , has recently been found to be quasilinear (C_2 symmetry) in its \tilde{X}^3B ground state,⁴³ with a deformed chain structure which is similarly suggested for HC_5H in the $1^3\Sigma_u^-$ state.

A UV band system of another C_5H_2 isomer was also measured in the matrix. It is assigned to the strong $1^1A_1 \leftarrow \tilde{X}^1A_1$ transition of pentatetraenylidene H_2CCCCC (**B**) based on calculated excitation energies and Franck-Condon simulations of the most stable isomers.

TABLE IV. Electronic transitions of $C_5H_2^+$ isomers below 6 eV predicted with the MS(6)-CASPT2(11/12)/cc-pVTZ method using ground state geometries from M06-2X/cc-pVTZ calculations.

B ⁺ \tilde{X}^2B_2		D ⁺ \tilde{X}^2A'		F ⁺ \tilde{X}^2A'	
State [eV]	<i>f</i>	State [eV]	<i>f</i>	State [eV]	<i>f</i>
1^2B_2	2.59 0.001	$1^2A'$	3.01 0.029	$1^2A'$	1.00 0.001
2^2B_2	3.01 0.001	$2^2A'$	4.31 0.001	$3^2A'$	3.11 0.001
3^2B_2	3.50 0.007	$3^2A'$	5.19 0.002		
4^2A_1	4.52 0.002	$4^2A'$	5.48 0.17		
1^2A_2	1.87 0.002	$1^2A''$	3.02 0.001		
2^2A_2	2.41 0.004	$3^2A''$	4.47 0.001		
3^2A_2	4.40 0.001	$5^2A''$	5.76 0.002		
4^2A_2	4.91 0.002				
5^2A_2	5.25 0.006				

TABLE V. Observed absorption maxima (cm^{-1}) in the $1^1A_1 \leftarrow \tilde{X}^1A_1$ electronic spectrum of H_2CCCCC in a neon matrix and proposed assignment.

$\tilde{\nu}$	$\Delta\tilde{\nu}$	Assignment
33000	0	0_0^0
33140	140	15_0^2
33890	890	6_0^1
34830	1830	$3_0^1, 6_0^2$
35860	2860	$3_0^1 6_0^1, 6_0^3$
36740	3740	$3_0^2, 3_0^1 6_0^2, 6_0^4$

ACKNOWLEDGMENTS

This work has been funded by the Swiss National Science Foundation (Project 200020-140316/1).

- ¹S. T. Ridgway, D. N. B. Hall, R. S. Wojslaw, S. G. Kleinmann, and D. A. Weinberger, *Nature* **264**, 345 (1976).
- ²V. G. Kunde, A. C. Aikin, R. A. Hanel, D. E. Jennings, W. C. Maguire, and R. E. Samuelson, *Nature* **292**, 686 (1981).
- ³S. J. Kim, J. Caldwell, A. R. Rivolo, and R. Wagener, *Icarus* **64**, 233 (1985).
- ⁴J. Cernicharo, A. M. Heras, A. G. G. M. Tielens, J. R. Pardo, F. Herpin, M. Guélin, and L. B. F. M. Waters, *Astrophys. J. Lett.* **546**, L123 (2001).
- ⁵K. H. Hinkle, J. J. Keady, and P. F. Bernath, *Science* **241**, 1319 (1988).
- ⁶J. P. Maier, N. M. Lakin, G. A. H. Walker, and D. A. Bohlender, *Astrophys. J.* **553**, 267 (2001).
- ⁷P. F. Bernath, K. H. Hinkle, and J. J. Keady, *Science* **244**, 562 (1989).
- ⁸P. Thaddeus, C. A. Gottlieb, A. Hjalmarsen, L. E. B. Johansson, W. M. Irvine, P. Friberg, and R. A. Linke, *Astrophys. J. Lett.* **294**, L49 (1985).
- ⁹J. Cernicharo, C. Kahane, J. Gómez-González, and M. Guélin, *Astron. Astrophys.* **164**, L1 (1986).
- ¹⁰M. Guélin, J. Cernicharo, M. J. Travers, M. C. McCarthy, C. A. Gottlieb, P. Thaddeus, M. Ohishi, S. Saito, and S. Yamamoto, *Astron. Astrophys.* **317**, L1 (1997).
- ¹¹J. Fulara, P. Freivogel, D. Forney, and J. P. Maier, *J. Chem. Phys.* **103**, 8805 (1995).

- ¹²C. D. Ball, M. C. McCarthy, and P. Thaddeus, *Astrophys. J. Lett.* **523**, L89 (1999).
- ¹³C. D. Ball, M. C. McCarthy, and P. Thaddeus, *J. Chem. Phys.* **112**, 10149 (2000).
- ¹⁴H. Ding, T. W. Schmidt, T. Pino, A. E. Boguslavskiy, F. Güthe, and J. P. Maier, *J. Chem. Phys.* **119**, 814 (2003).
- ¹⁵S. C. Madden, W. M. Irvine, H. E. Matthews, P. Friberg, and D. A. Swade, *Astron. J.* **97**, 1403 (1989).
- ¹⁶J. M. Vrtilik, C. A. Gottlieb, E. W. Gottlieb, T. C. Killian, and P. A. Thaddeus, *Astrophys. J. Lett.* **364**, L53 (1990).
- ¹⁷J. A. Hodges, R. J. McMahon, K. W. Sattelmeyer, and J. F. Stanton, *Astrophys. J.* **544**, 838 (2000).
- ¹⁸E. Achkasova, M. Araki, A. Denisov, and J. P. Maier, *J. Mol. Spectrosc.* **237**, 70 (2006).
- ¹⁹J. P. Maier, G. A. H. Walker, D. A. Bohlender, F. J. Mazzotti, R. Raghunandan, J. Fulara, I. Garkusha, and A. Nagy, *Astrophys. J.* **726**, 41 (2011).
- ²⁰R. A. Seburg, R. J. McMahon, J. F. Stanton, and J. Gauss, *J. Am. Chem. Soc.* **119**, 10838 (1997).
- ²¹S. J. Blanksby, S. Dua, J. H. Bowie, D. Schröder, and H. Schwarz, *J. Phys. Chem. A* **102**, 9949 (1998).
- ²²A. Mavrandonakis, M. Mühlhauser, G. E. Froudakis, and S. D. Peyerimhoff, *Phys. Chem. Chem. Phys.* **4**, 3318 (2002).
- ²³M. C. McCarthy, M. J. Travers, A. Kovacs, W. Chen, S. E. Novick, C. A. Gottlieb, and P. Thaddeus, *Science* **275**, 518 (1997).
- ²⁴M. J. Travers, M. C. McCarthy, C. A. Gottlieb, and P. Thaddeus, *Astrophys. J. Lett.* **483**, L135 (1997).
- ²⁵C. A. Gottlieb, M. C. McCarthy, V. D. Gordon, J. M. Chakan, A. J. Apponi, and P. Thaddeus, *Astrophys. J. Lett.* **509**, L141 (1998).
- ²⁶N. P. Bowling, R. J. Halter, J. A. Hodges, R. A. Seburg, P. S. Thomas, C. S. Simmons, J. F. Stanton, and R. J. McMahon, *J. Am. Chem. Soc.* **128**, 3291 (2006).
- ²⁷P. Freivogel, J. Fulara, D. Lessen, D. Forney, and J. P. Maier, *Chem. Phys.* **189**, 335 (1994).
- ²⁸Y. Zhao and D. G. Truhlar, *Theor. Chem. Acc.* **120**, 215 (2008).
- ²⁹T. H. Dunning, *J. Chem. Phys.* **90**, 1007 (2003).
- ³⁰D. E. Woon and T. H. Dunning, *J. Chem. Phys.* **98**, 1358 (1993).
- ³¹M. J. Frisch, G. W. Trucks, H. B. Schlegel, G. E. Scuseria, M. A. Robb, J. R. Cheeseman, G. Scalmani, V. Barone, B. Menucci, G. A. Petersson, H. Nakatsuji, M. Caricato, X. Li, H. P. Hratchian, A. F. Izmaylov, J. Bloino, G. Zheng, J. L. Sonnenberg, M. Hada, M. Ehara, K. Toyota, R. Fukuda, J. Hasegawa, M. Ishida, T. Nakajima, Y. Honda, O. K. H. Nakai, T. Vreven, J. A. Montgomery, J. E. Peralta, F. Ogliaro, M. Bearpark, J. J. Heyd, E. Brothers, K. N. Kudin, V. N. Staroverov, T. Keith, R. Kobayashi, J. Normand, K. Raghavachari, A. Rendell, J. C. Burant, S. S. Iyengar, J. Tomasi, M. Cossi, N. Rega, J. M. Millam, M. Klene, J. E. Knox, J. B. Cross, V. Bakken, C. Adamo, J. Jaramillo, R. Gomperts, R. E. Stratmann, O. Yazyev, A. J. Austin, R. Cammi, C. Pomelli, J. W. Ochterski, R. L. Martin, K. Morokuma, V. G. Zakrzewski, G. A. Voth, P. Salvador, J. J. Dannenberg, S. Dapprich, A. D. Daniels, O. Farkas, J. B. Foresman, J. V. Ortiz, J. Cioslowski, and D. J. Fox, "Gaussian 09, revision d.01," Tech. Rep. (Wallingford, CT: Gaussian, Inc., 2013).
- ³²F. Aquilante, L. D. Vico, N. Ferré, G. Ghigo, P. Malmqvist, P. Neogrády, T. B. Pedersen, M. Pitonak, M. Reiher, B. O. Roos, L. Serrano-Andrés, M. Urban, V. Veryazov, and R. Lindh, *J. Comput. Chem.* **31**, 224 (2010).
- ³³H. Nakatsuji and K. Hirao, *J. Chem. Phys.* **68**, 2053 (1978).
- ³⁴H. Nakatsuji, *Chem. Phys. Lett.* **68**, 329 (1979).
- ³⁵C. M. Western, "Pgopher, version 7.1.108," Tech. Rep. (University of Bristol, <http://pgopher.chm.bris.ac.uk>, 2010).
- ³⁶A. D. Becke, *Phys. Rev. A* **38**, 3098 (1988).
- ³⁷C. Lee, W. Yang, and R. G. Parr, *Phys. Rev. B* **37**, 785 (1988).
- ³⁸J. Fulara, A. Nagy, I. Garkusha, and J. P. Maier, *J. Chem. Phys.* **133**, 024304/1 (2010).
- ³⁹J. Fulara, A. Chakraborty, A. Nagy, K. Filipkowski, and J. P. Maier, *J. Phys. Chem. A* **119**, 2338 (2015).
- ⁴⁰The CASPT2 method implemented in MOLCAS allows the computation of only totally symmetric vibrations.
- ⁴¹A. Chakraborty, J. Fulara, R. Dietsche, and J. P. Maier, *Phys. Chem. Chem. Phys.* **16**, 7023 (2014).
- ⁴²J. Cernicharo, M. Guélin, and C. M. Walmsley, *Astron. Astrophys.* **172**, L5 (1987).
- ⁴³D. L. Osborn, K. M. Vogelhuber, S. W. Wren, E. M. Miller, Y.-J. Lu, A. S. Case, L. Sheps, R. J. McMahon, J. F. Stanton, L. B. Harding, B. Ruscic, and W. C. Lineberger, *J. Am. Chem. Soc.* **136**, 10361 (2014).